SCIENTIFIC REPORTS

OPEN

SUBJECT AREAS:
PLASMA-BASED ACCELERATORS
LASER-PRODUCED PLASMAS

Received
14 April 2014

Accepted
22 July 2014

Published
8 August 2014

Correspondence and requests for materials should be addressed to M.K. (mkrism@tifr.res.in)

Bacterial cells enhance laser driven ion acceleration

Malay Dalui[1], M. Kundu[2], T. Madhu Trivikram[1], R. Rajeev[1], Krishanu Ray[1] & M. Krishnamurthy[1,3]

[1]Tata Institute of Fundamental Research, 1 Homi Bhabha Road, Colaba, Mumbai 400 005, India, [2]Institute for Plasma Research, Bhat, Gandhinagar 382 428, India, [3]TIFR Centre for Interdisciplinary Sciences, 21 Brundavan Colony, Narsingi, Hyderabad 500075, India.

Intense laser produced plasmas generate hot electrons which in turn leads to ion acceleration. Ability to generate faster ions or hotter electrons using the same laser parameters is one of the main outstanding paradigms in the intense laser-plasma physics. Here, we present a simple, albeit, unconventional target that succeeds in generating 700 keV carbon ions where conventional targets for the same laser parameters generate at most 40 keV. A few layers of micron sized bacteria coating on a polished surface increases the laser energy coupling and generates a hotter plasma which is more effective for the ion acceleration compared to the conventional polished targets. Particle-in-cell simulations show that micro-particle coated target are much more effective in ion acceleration as seen in the experiment. We envisage that the accelerated, high-energy carbon ions can be used as a source for multiple applications.

High intensity laser-driven proton and ion acceleration is a rapidly growing research field with possible applications in proton therapy[1], multi-MeV ion beam production[2–5] and proton radiography[6]. The ability to use intense ultra-short pulses to generate high energy ion pulses with high peak current is important not only from the fundamental view point but also towards developing novel applications. For example, laser accelerated proton beam is chirped where the faster protons stay at the front of the bunch followed by the slower protons. Such properties enables continuous time evolution measurements[7,8]. Protons and ions are promising alternatives in fast ignition[9,10] for inertial confinement fusion because of simpler interaction with the hot dense plasma and near-ballistic propagation[11]. Ultra-short high intensity laser field rapidly ionizes the matter and the subsequent collective process of plasma heating leads to the generation of energetic electrons, which eventually leave the target surface. Local charge imbalance created due to this rapid electron ejection from the target surface which gives rise to a quasi-static electric field which accelerates the ions[12–16]. Thus, immediately following the hot electrons, atomic ions formed on the target surface are accelerated by the conversion of the induced electrostatic field energy into the ion kinetic energy. The quasi-static charge separation sheath electric field, generated by the laser produced hot electrons at the interface of the target and the vacuum, which accelerates the ions is given in the formula below[13]:

$$E_{sheath} = \left(\frac{2k_B n_{eh} T_{eh}}{e\varepsilon_0}\right)^{1/2} \quad (1)$$

where, k_B is the Boltzmann constant, e is the charge of an electron, ε_0 is the free space permittivity, n_{eh} is the hot electron density and T_{eh} is the hot electron temperature. Hence, the strength of the charge separation sheath field depends on the hot electron density and its temperature. The maximum ion energy is decided by the strength of E_{sheath}. By increasing n_{eh} and T_{eh}, the sheath field becomes larger and the maximum ion energy can be increased for a given laser intensity.

The accelerating gradient achieved in a typical laser-plasma based ion accelerators is of the order of TV/m. In the laser-plasma experiments involving solid targets, hydrogen and lighter atoms, such as, carbon and oxygen always exist in the form of hydrocarbon contaminants on the target surface, and they yield predominant high energy ion signals due to their higher charge-to-mass ratio (q/m) as compared to other heavier ions. The interaction of an obliquely incident p-polarized intense short laser pulse with a polished solid target channelizes 30-40% of the light energy to the electrons[17,18]. However, it has been reported that the light absorption can be enhanced by engineering suitable modulation on the target surface[19–24]. The enhanced light absorption boosts the hot electron population and increases their temperature, which can lead to a higher sheath field (E_{sheath}). This in turn is expected to influence a more efficient ion acceleration[25–27]. Previous studies with certain targets, surface

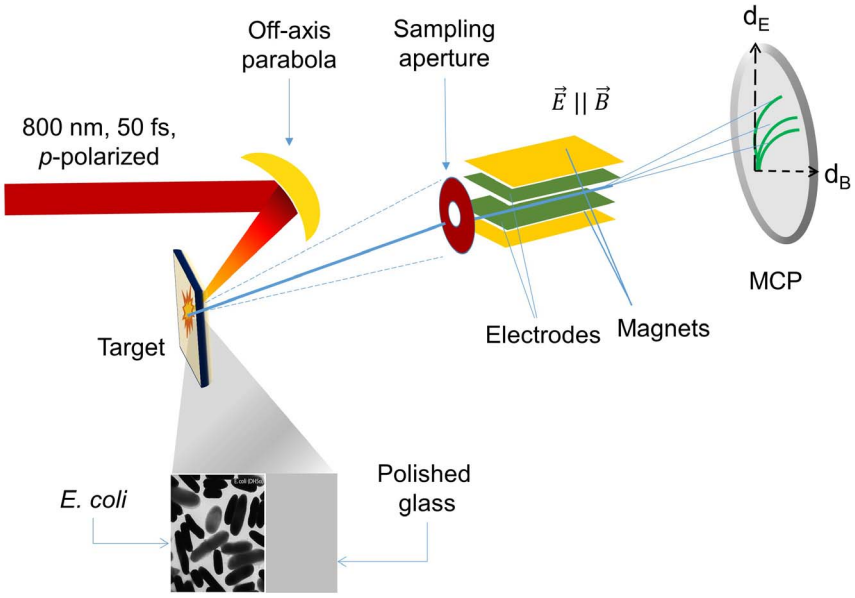

Figure 1 | Schematic of the experiment. A 800 nm, 50 fs laser pulse is focused, using an off-axis parabolic mirror, on the target. Inset shows the target surface geometry. Ions were detected using a Thomson parabola spectrometer at the target normal direction. d_E and d_B are the deflections of the charged particles due to the parallel electric and the magnetic field respectively. The TP was kept in a differentially pumped chamber maintained at a pressure of 10^{-7} torr, while the main experimental chamber was at 6×10^{-5} torr pressure.

modulated with nano-structuring has achieved a 13 fold enhancement in bremsstrahlung x-ray emission as compared to a polished surface[22]. However, it is two orders of magnitude higher from the bacteria (micro-particles) coated target[24]. A 2.5 times increase in T_{eh} was also observed in this case. We may now envisage that, if a bacteria coated target is used for the ion acceleration, the maximum ion energies can be increased more than 10 times, if a 100 fold increase in the electron density is assumed (from the knowledge of two orders increment in the x-ray flux), in accordance with the above mentioned simple and well established formalism (equation 1).

The ion acceleration studies with structured targets broadly concentrate on the proton acceleration and do not conclusively prove whether target structuring of dimensions of the order of the laser wavelength improves the ion acceleration[26,27]. Moreover, the effect of micro-structuring on the majority of the ionic species (proton, carbon, oxygen etc) is hardly explored. In this paper we address these issues. We report a study on the ion emission from an optically polished target and a bacteria coated target. Half of a polished BK-7 glass substrate is coated with a few layers of ellipsoidal ($\sim$1.8 μm × $\sim$0.7 μm) *E. coli* bacteria cells. We find that, for the same laser intensity and other pulse parameters, the bacteria coated target yields carbon ions with a maximum ion energy up to 700 keV, while the plain polished substrate, which can be taken as the reference to the ion acceleration from conventional targets, yields a maximum of only 40 keV carbon ions. To justify the experimental observations we have performed fully relativistic two-dimensional electro-magnetic particle-in-cell simulations assuming bacteria as ellipsoidal micro-particles of appropriate dimensions. Simulations do show that the electric field, experienced by the ions in the sheath, is larger with the bacteria cell coating and the experimental ion energy measurements can be fully comprehended with the simulation. In addition to the carbon ions, protons also get accelerated. We note that, the maximum proton energy does not show similar enhancement as carbon ions. However, this can be explained based on the arguments about the initial spread of the easily movable protons (owing to its highest q/m amongst the ions) in space and is well demonstrated by additional hydrodynamic simulations. Results presented here gives a fresh impetus to tune intense laser produced plasmas for effective acceleration of heavier ions apart from the proton acceleration.

Results

The experiment was performed using a Ti:Sapphire laser and the ions were detected at the target-front normal using a Thomson Parabola (TP) Spectrometer[28] as shown in figure 1. The TP ion traces and the corresponding energy spectra for the carbon ions are shown in figure 2. The image shows that the dominant ions with the bacteria coated glass and the plain glass substrate are of carbon, oxygen and protons. Both the targets also show signal due to ions of higher atomic number (Z $\sim$ 10). Carbon and oxygen have very close charge-to-mass ratios (q/m) and behave similarly. Oxygen ion energies are always found to show very similar behavior though the maximum ion energies are lower than the carbon ions. Thus, the acceleration features are summarized only with the analysis of carbon ions and other heavier ions are ignored in the present study. Protons on the other hand respond differently and its acceleration features are also presented in detail. Each ionic species, light or heavy, show a sharp cut-off towards the highest energy end in their respective kinetic energy spectra. This cut-off originates from the fact that the accelerated ions eventually catch up with the electrons, which inhibits further acceleration. Previous studies by Krishnamurthy *et al*, using the similar micro-particle system reported 70 fold enhancement in the hot electron production with 2.5 times increment in the hot electron temperature as compared to polished targets[24]. If we make a simple assumption that the 70 fold enhancement in the hot electron emission essentially correlates to an effective increase in the electron density, which increases the effective accelerating electrostatic sheath. Hence, the accelerating field is stronger by $(\sqrt{70 \times 2.5})$ (see equation 1) about 13 times. The maximum ion energy of the charge particles accelerated in such a sheath would be 13 times larger. We should keep in mind that, it is a very simplistic representation of a very complex phenomenon since the electron density is a strong function of both space and time and the dynamical evolution of the sheath with micro-particle structures can be very different. The simplistic picture, however, indicates that the maximum ion energy can be more than ten-fold larger if the ions are accelerated in such an enhanced electrostatic sheath field.

Figure 2c shows the comparison of the carbon ion energy spectra from the polished (glass) and the *E. coli* coated target. We did not observe any measurable signal of C^{3+} from glass indicating that the

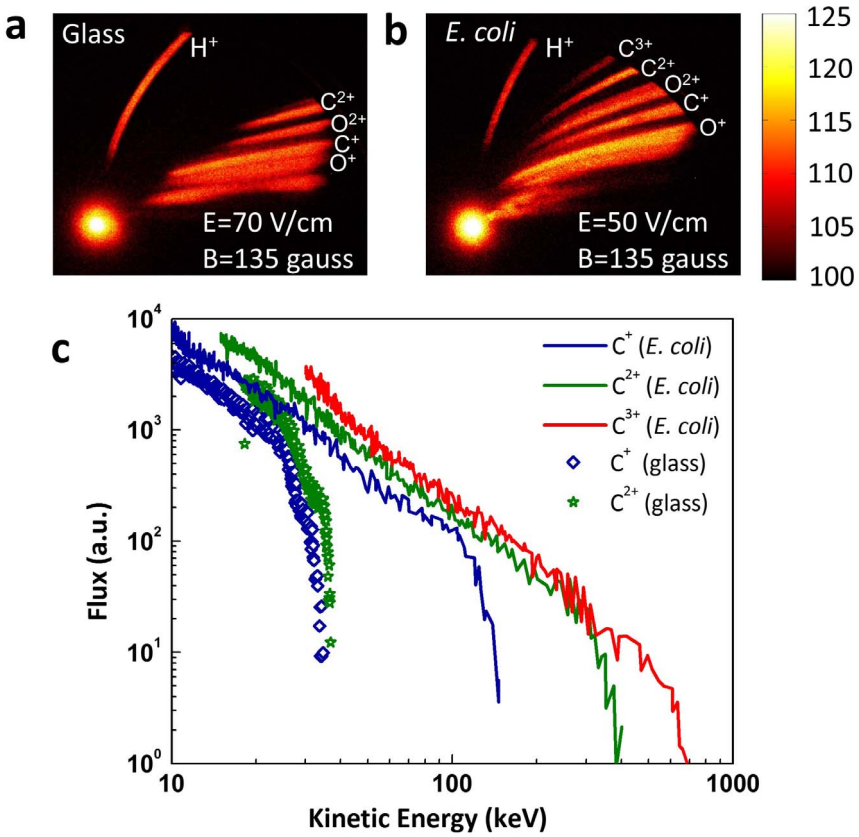

Figure 2 | **Ion spectrometric measurements.** Thomson parabola images of the ions and the energy spectra of the carbon ions observed with a focused laser intensity of 5×10^{17} W/cm^2. **a** and **b** are the TP images from glass and *E. coli* cells respectively. Horizontal axis gives the deflection due to the electric field (d_E) and the vertical axis is due to the deflection by the magnetic field (d_B) in the TP. **c** is the carbon ion energy spectra obtained for the TP image.

ionization strength is lower in the polished glass target. With Bacteria coating, C^{2+} and C^{3+} show much higher energies where the maximum ion energy extends to 400 and 700 keV respectively. This is more than an order of magnitude larger compared to polished targets where the highest energy is only about 30–40 keV. This clearly demonstrates that the simple analysis of expecting more than ten-fold enhancement is well observed in the experiment. However, to fully comprehend the enhanced coupling of the laser energy due to the bacteria coating and its effect on the ion acceleration, we have performed fully-relativistic two-dimensional particle-in-cell (PIC) simulations.

In the PIC simulation, *E. coli* bacteria are modelled as ellipsoidal micro-particles of size 0.7 μm × 1.8 μm to mimic the experimental target surface geometry. Thus, we consider two different kind of targets: (i) elliptical micro-particles distributed on a solid slab, and (ii) a plain solid slab (without micro-particles) which compares to the glass substrate. The chosen targets are then illuminated with a pulsed Gaussian light beam of wavelength $\lambda = 800$ nm. Numerical simulations are performed on a 1000 × 1000 rectangular grids with a uniform grid size of $\Delta = \lambda/40$, and a time step of $\delta t = \Delta/2c$ (c is the speed of light) to have convergent solution and negligible numerical heating. The angle of incidence of the light pulse is controlled by rotating the target about an axis (y-axis) which is normal to the plane of incidence (x-z-plane, with z being the propagation and x being the polarization direction). In the simulation, the peak intensity, pulse width and the angle of incidence of the laser beam are taken as used in the experiment. Though the real target system has carbon, oxygen and protons, it is very difficult to simulate the exact target compositions in the PIC simulation as spatial variations of several species and their density distributions are not known exactly. We consider the target to be composed of only hydrogen (proton) for both the slab and the ellipsoidal micro-particles such that the essential differences in the ion acceleration with the change in the target features are deciphered. Since *E. coli* bacteria has more than 90% water content, we consider uniform initial electron density of $2n_c$ for ellipsoidal particles, and $10n_c$ for the solid slab (substrate) respectively, where, $n_c \approx 1.72 \times 10^{21}$ cm^{-3} is the critical electron density at a wavelength $\lambda = 800$ nm. Figure 3 shows the simulated proton energy spectra from the solid slab and the elliptical micro-particles coated solid slab.

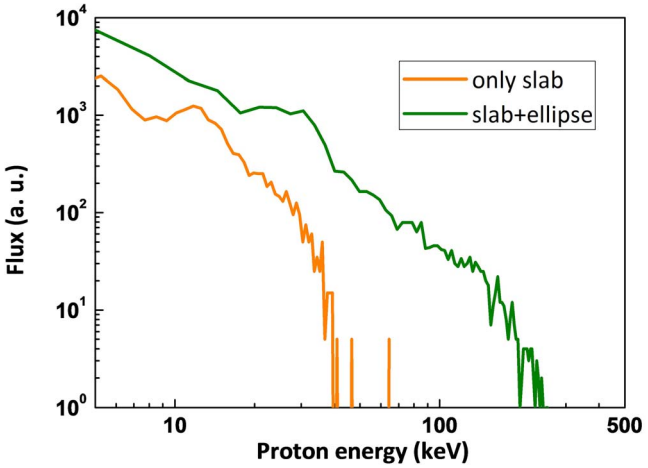

Figure 3 | **PIC simulations.** The proton energy spectra from the polished and ellipse coated target computed using particle-in-cell simulations. The enhanced sheath field formed with the micro-particle coating brings forth almost 10 fold increase in the maximum ion energy.

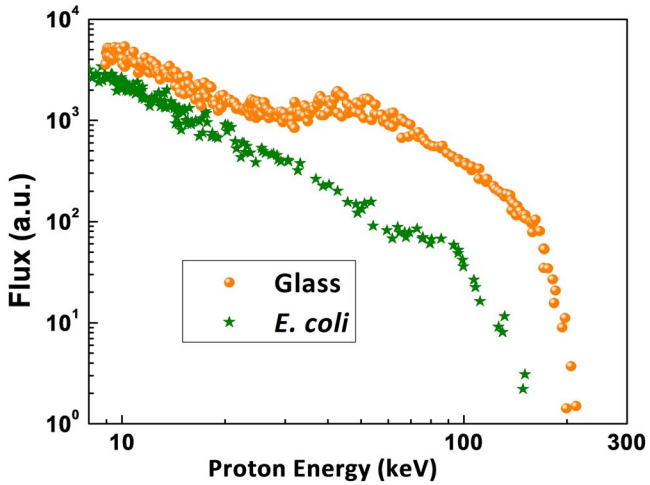

Figure 4 | Proton energy measurements. Energy spectra of the protons derived from the TPS ion traces (figure 2a and 2b).

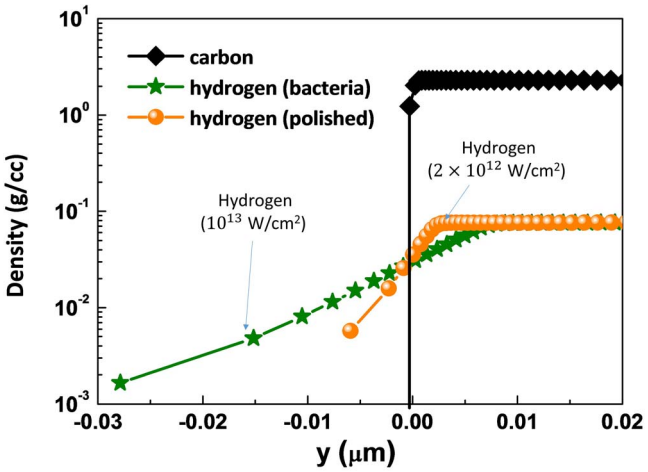

Figure 5 | MULTI-fs hydrodynamic simulation results. Dotted lines represent the carbon expansion from the polished target surface, which cannot be seen as it overlaps with the scatter plot. Spheres and asterisks show the hydrogen expansion from the polished glass and the microstructured target respectively.

The result is plotted after the simulation is run for 66 fs. The simulation result very clearly demonstrates the generation of much higher energy ions with elliptical micro-particles or bacteria coated target compared to the plain solid slab target. The maximum ion energy is nearly ten times larger with the microstructured target much like the experimental measurements shown in figure 2c. The presence of the microstructure thus increases the laser energy absorption and the generation of hotter electrons. Enhanced hot electron generation in turn brings forward a stronger sheath electric field and facilitates with better ion acceleration.

The TP image also depicts a strong proton signal from both the targets. A comparison of the proton signals from both the targets is shown in figure 4. The maximum proton energy with the micro-particle coated target is not larger than the plain glass target, which is an apparent deviation from the analysis presented thus far. This anomaly in the proton acceleration in the *E. coli* coated target is because of the different expansion of hydrogen and carbon prior to the arrival of the main femtosecond laser pulse and is elaborated below.

The real ultra-short laser pulses are not delta functions in time and generally have low energy wings, (pre-pulse and post-pulse) due to a non-zero value of the ASE[29] (amplified spontaneous emission). The pre-pulse interacts much before the peak pulse arrives to the target. The ASE to the main pulse intensity contrast ratio for the current experiment is 5×10^{-6} at a few picoseconds. The weak pre-pulse can ionize the target and set the ions in motion. In this case, protons would start moving much before the arrival of the main intense laser pulse and would move a larger distance compared to carbon. Due to the scattering of light, the local fields are 4–5 times larger with a micro-particle coated target compared to the plain polished target. So, in bacterial targets where the local fields are larger even for the pre-pulse, the pre-ionization and proton motion are more prominent. Thus, in a bacterial target the protons move away much more from the target surface than that of the plain polished target and hence they do not experience the full sheath potential. Therefore, the proton energy is reduced in the bacteria target compared to the carbon ions for the negligible expansion of the later species. To place these arguments in a more quantitative way MULTI-fs hydrodynamic simulation[30] has been performed to understand the changes in the spatial profile of the target density.

In the simulations, a constant pulse of 1 ns temporal duration propagating from the left to the right along the y-axis is taken to represent the pre-pulse (ASE). The target is a 25 μm thick solid substrate (made up of either hydrogen or carbon). The material density of hydrogen and carbon are taken to be 0.076 g/cc and 2.2 g/cc respectively. The pre-pulse intensity on the polished hydrogen and the carbon target is 2×10^{12} W/cm^2. The micro-particle coated target is modelled as flat surface with a higher pre-pulse intensity (10^{13} W/cm^2) to correspond to 5 times larger local fields generated in these targets. Figure 5 shows the ion density along the laser propagation direction for different kinds of targets, before the interaction of the main pulse. When the target is made up of only carbon, it suffers no difference due to the higher pre-pulse intensity. On the other hand for the target with the hydrogen there is a very noticeable motion of the hydrogen. The higher expansion of hydrogen prior to the arrival of the main fs pulse, due to the enhanced local fields in the micro-particle coated target would reduce the accelerating length and the electro-static sheath field experienced by these ions. So, the carbon ion expansion is negligible and hence, these ions are accelerated efficiently in the enhanced electro-static sheath.

Discussion

We find that a few monolayers of micron sized *E. coli* cells (essentially a bag of water packed in elliptical shapes) coated on a plain polished glass dramatically alters the ion acceleration when exposed to 50 fs laser pulses focused to an intensity of 5×10^{17} W/cm^2. Carbon ions with maximum energy up to 700 keV are measured with a Thompson Parabola spectrometer while the conventional polished glass target generates ions only up to 40 keV under identical conditions yielding almost 18-fold enhancement. Particle-in-cell simulations, carried out with elliptical particles placed on a solid slab, clearly shows that the ion energy is larger with the *E. coli* coating than that of the plain solid slab. Computed proton spectrum clearly shows the formation of a stronger electrostatic sheath with the introduction of the micro particles, giving almost 10-fold enhanced maximum ion energy in good agreement with the experimental measurements. The TP measurements of the proton spectrum however indicate that the maximum proton energy is less with the bacteria coating. This apparent discrepancy can very well be explained if we consider the motion of the protons due to the pre-pulse. The present experimental observation is an excellent example to avoid the discrepancy by considering only protons to judge the strength of the hot electron sheath field. It is evident that the bacteria coating increases the sheath field and the carbon ions are accelerated very effectively. This work would give a new impetus to engineer targets for enhanced heavy ion acceleration for a given laser intensity.

Methods

A 50 fs, Ti:Sapphire, CPA laser of 800 nm central wavelength operating at 10 Hz repetition rate was used for the experiment. The *p*-polarized laser beam was focused using an f/4 off-axis parabolic mirror (OAP) to a 12 μm spot at 40° angle of incidence yielding a peak intensity of 5×10^{17} W/cm^2. The ion emission was recorded at the target-front normal using a Thomson Parabola Spectrometer equipped with a micro-channel-plate (MCP) placed at 1.3 m away from the laser focus[28]. The image of the phosphor screen at the end of the MCP was collected by a CCD camera. A TP distinctively separates kinetic energy spectrum from a broad distribution of multiply charged ions according to their charge-to-mass ratio[31] (q/m). It maps the kinetic energy of a particular q/m into a parabolic trace on the MCP. The parallel electric and the magnetic field arrangements deflect the ions in the plane perpendicular to their velocity. The ion beam was extracted through a 100 μm aperture placed well before the field region of the TP. One half portion of a λ/10 polished BK-7 glass substrate was coated with few monolayer of *E. coli* cells and the intense laser pulses were focused either on the bacteria coated glass or on the plain glass under otherwise identical conditions. Details of the target preparation are elaborated in our previous work[24]. Light ions are always present on BK-7 as surface contamination and 95% of the *E. coli* is made up with water. *E. coli*, being micro-structured, modifies the target surface and enhances the light absorption. TP ion traces are collected from both the targets in identical experimental conditions.

1. Malka, V. *et al.* Practicability of protontherapy using compact laser systems., *Med. Phys.* **31**, 1587 (2004).
2. Krushelnick, K. *et al.* Multi-MeV Ion Production from High-Intensity Laser Interactions with Underdense Plasmas. *Phys. Rev. Lett.* **83**, 737 (1999).
3. Maksimchuk, A., Gu, S., Flippo, K., Umstadter, D. & Bychenkov, V. Yu. Forward Ion Acceleration in Thin Films Driven by a High-Intensity Laser. *Phys. Rev. Lett.* **84**, 4108 (2000).
4. Clark, E. L. *et al.* Measurements of Energetic Proton Transport through Magnetized Plasma from Intense Laser Interactions with Solids. *Phys. Rev. Lett.* **84**, 670 (2000).
5. Snavely, R. A. *et al.* Intense High-Energy Proton Beams from Petawatt-Laser Irradiation of Solids. *Phys. Rev. Lett.* **85**, 2945 (2000).
6. Borghesi, M. *et al.* Laser-produced protons and their application as a particle probe. *Laser and Particle Beams* **20**, 269 (2002).
7. Borghesi, M. *et al.* Proton imaging: a diagnostic for inertial confinement fusion/fast ignitor studies. *Plasma Phys. Control Fusion* **43**, A267 (2001).
8. Sokollik, T. *et al.* Transient electric fields in laser plasmas observed by proton streak deflectometry. *Appl. Phys. Lett.* **92**, 091503 (2008).
9. Roth, M. *et al.* Fast Ignition by Intense Laser-Accelerated Proton Beams. *Phys. Rev. Lett.* **86**, 436 (2001).
10. Atzeni, S., Temporal, M. & Honrubia, J. J. A first analysis of fast ignition of precompressed ICF fuel by laser-accelerated protons. *Nucl. Fusion* **42**, L1–L4 (2002).
11. Sentoku, Y. *et al.* High density collimated beams of relativistic ions produced by petawatt laser pulses in plasmas. *Phys. Rev. E* **62**, 7271 (2000).
12. Wilks, S. C. *et al.* Energetic proton generation in ultra-intense laser-solid interactions. *Phys. plasmas* **8**, 542 (2001).
13. Mora, P. Plasma Expansion into a Vacuum. *Phys. Rev. Lett.* **90**, 185002 (2003).
14. Passoni, M., Tikhonchuk, V. T., Lontano, M. & Bychenkov, V. Yu. Charge separation effects in solid targets and ion acceleration with a two-temperature electron distribution. *Phys. Review E* **69**, 026411 (2004).
15. Mora, P. Thin-foil expansion into a vacuum. *Phys. Review E* **72**, 056401 (2005).
16. Murakami, M. & Basko, M. M. Self-similar expansion of finite-size non-quasi-neutral plasmas into vacuum: Relation to the problem of ion acceleration. *Phys. Plasmas* **13**, 012105 (2006).
17. Hatchett Stephen, P. *et al.* Electron, photon, and ion beams from the relativistic interaction of Petawatt laser pulses with solid targets. *Phys. Plasmas* **7**, 2076 (2000).
18. Kruer, W. L. *The Physics of Laser Plasma Interaction* (Westview press, Colorado, 2003).
19. Murnane, M. M. *et al.* Efficient coupling of high-intensity subpicosecond laser pulses into solids. *Appl. Phys. Lett.* **62**, 1068 (1993).
20. Nishikawa, T. *et al.* Greatly enhanced soft x-ray generation from femtosecond-laser-produced plasma by using a nanohole-alumina target. *Appl. Phys. Lett.* **75**, 4079 (1999).
21. Kulcsar, G. *et al.* Intense Picosecond X-Ray Pulses from Laser Plasmas by Use of Nanostructured "Velvet" Targets. *Phys. Rev. Lett.* **84**, 5149 (2000).
22. Rajeev, P. P. *et al.* Metal Nanoplasmas as Bright Sources of Hard X-Ray Pulses. *Phys. Rev. Lett.* **90**, 115002 (2003).
23. Klimo, O. *et al.* Short pulse laser interaction with micro-structured targets: simulations of laser absorption and ion acceleration. *New J. Physics* **13**, 053028 (2011).
24. Krishnamurthy, M. *et al.* A bright point source of ultrashort hard x-ray pulses using biological cells. *Optics Express* **20**, 5754 (2012).
25. Zigler, A. *et al.* 5.5–7.5 MeV Proton Generation by a Moderate-Intensity Ultrashort-Pulse Laser Interaction with H_2O Nanowire Targets. *Phys. Rev. Lett.* **106**, 134801 (2011).
26. Margarone, D. *et al.* Laser-Driven Proton Acceleration Enhancement by Nanostructured Foils. *Phys. Rev. Lett.* **109**, 234801 (2012).
27. Zigler, A. *et al.* Enhanced Proton Acceleration by an Ultrashort Laser Interaction with Structured Dynamic Plasma Targets. *Phys. Rev. Lett.* **110**, 215004 (2013).
28. Dalui, M., Madhu Trivikram, T., Ram Gopal & Krishnamurthy, M. Probing strong field ionization of solids with a Thomson parabola spectrometer. *Pramana–J. Phys.* **82**, 111 (2014).
29. Diels, J. C. & Rudolph, W. *Ultrashort Laser Pulse Phenomena* (Elsevier Inc. 2006).
30. Ramis, R., Eidmann, K., Meyer-ter-Vehn, J. & Hüller, S. MULTI-fs- A Compact Code for Laser-Plasma Interaction in the Femtosecond Regime. *Computer Physics Communications* **183**, 637 (2012).
31. Thomson, J. J. Rays of positive electricity. *Proceedings of the Royal Society A* **89**, 1–20 (1913).

Acknowledgments

M.K. thanks the swarnajayanthi fellowship of the Govt. of India. The author thank K.P.M. Risad, Prashant Kumar Singh for initial help in this work.

Author contributions

M.K. conceived the idea of ion acceleration using the bacteria cells in discussion with K.R. and M.D. The experiments were performed by M.D. and T.M.T. Sample preparation was done by K.R. Kundu carried out the PIC simulations. R.R. contributed in data analysis along with M.D. and T.M.T. The hydrodynamic simulation was carried out by M.D. The manuscript was written by M.K., M.D. and Kundu. All authors have reviewed the manuscript.

Additional information

Competing financial interests: The authors declare no competing financial interests.

How to cite this article: Dalui, M. *et al.* Bacterial cells enhance laser driven ion acceleration. *Sci. Rep.* **4**, 6002; DOI:10.1038/srep06002 (2014).